Molecular genetics and quantitative traits divergence among populations of *Eothenomys miletus* from Hengduan Mountain region

Yue Ren[1], Ting Jia[2], Yanfei Cai[3], Lin Zhang[4], Hao Zhang[3], Zhengkun Wang[3], and Wanlong Zhu[3]

[1]Shanxi Agricultural University
[2]Yunnan University of Business Management
[3]Yunnan Normal University
[4]Hubei University of Chinese Medicine

January 16, 2023

Abstract

An important objective of evolutionary biology has always been to grasp the evolutionary and genetic processes that contribute to speciation. The present work provides the first detailed account of the genetic and physiological adaptation to changing environmental temperatures as well as the reasons causing intraspecific divergence in the *Eothenomys miletus* from the Hengduan mountain (HM) region, one of the biodiversity hotspots. 161 *E. miletus* individuals from five populations in the HM region had their genomes simplified sequenced, and one additional individual from each community had their genomes resequenced. We then characterized the genetic diversity and population structure of each population and compared the phenotypic divergence in traits using neutral molecular markers. We detected significant phenotypic and genetic alterations in *E. miletus* from the HM region that were related to naturally occurring diverse habitats by combining morphometrics and genomic techniques. The *E. miletus* existed asymmetric gene flow patterns, indicating that five *E. miletus* populations exhibit a isolation-by-island model, and this was supported by the correlation between FST and geographic distance. Finally, PST estimated by phenotypic measures of most wild traits were higher than differentiation at neutral molecular markers, indicating directional natural selection favouring different phenotypes in different populations must have been involved to achieve this much differentiation. Our findings give information on the demographic history of *E. miletus*, new insights into their evolution and adaptability, and literature for studies of a similar nature on other wild small mammals from the HM region.

Molecular genetics and quantitative traits divergence among populations of *Eothenomys miletus* from Hengduan Mountain region

Running title: Genomics and phenotypic adaptation of voles

Yue Ren[1, 2], Ting Jia[3], Yanfei Cai[1], Lin Zhang[4], Hao Zhang[1], Zhengkun Wang[1], Wanlong Zhu[1, 5, 6*]

1. Key Laboratory of Ecological Adaptive Evolution and Conservation on Animals-plants in Southwest Mountain Ecosystem of Yunnan Province Higher Institutes College, School of Life Sciences, Yunnan Normal University, Kunming, 650500, China; 2. College of Plant Protection, Shanxi Agricultural University, Taiyuan, 030024, China; 3. Yunnan College of Business Management, Kunming, 650106, China; 4. Hubei University of Chinese Medicine, Wuhan, 430065, China; 5. Engineering Research Center of Sustinable Development and Utilization of Biomass Energy Ministry of Education, Kunming, 650500, China; 6. Key Laboratory of Yunnan Province for Biomass Energy and Environment Biotechnology, Kunming, 650500, China.

***Correspondence author:** Dr. Wanlong Zhu, College of Life Sciences, Yunnan Normal University. 768 Juxian Street. Chenggong District, Kunming, 650500, China, China. E-mail: zwl_8307@163.com, Telephone number: 13759591394.

Molecular genetics and quantitative traits divergence among populations of *Eothenomys miletus* from Hengduan Mountain region

ABSTRACT:

An important objective of evolutionary biology has always been to grasp the evolutionary and genetic processes that contribute to speciation. The present work provides the first detailed account of the genetic and physiological adaptation to changing environmental temperatures as well as the reasons causing intraspecific divergence in the Eothenomys miletus from the Hengduan mountain (HM) region, one of the biodiversity hotspots. 161 *E. miletus* individuals from five populations in the HM region had their genomes simplified sequenced, and one additional individual from each community had their genomes resequenced. We then characterized the genetic diversity and population structure of each population and compared the phenotypic divergence in traits using neutral molecular markers. We detected significant phenotypic and genetic alterations in *E. miletu*s from the HM region that were related to naturally occurring diverse habitats by combining morphometrics and genomic techniques. The *E. miletus* existed asymmetric gene flow patterns, indicating that five *E. miletus* populations exhibit a isolation-by-island model, and this was supported by the correlation between F_{ST} and geographic distance. Finally, P_{ST} estimated by phenotypic measures of most wild traits were higher than differentiation at neutral molecular markers, indicating directional natural selection favouring different phenotypes in different populations must have been involved to achieve this much differentiation. Our findings give information on the demographic history of *E. miletus*, new

insights into their evolution and adaptability, and literature for studies of a similar nature on other wild small mammals from the HM region.

KEYWORDS: *Eothenomys miletus*, F_{ST} , genetic diversity, population genomic, P_{ST}

INTRODUCTION

Early flora and fauna cradleland and refuges are hotspots for biodiversity. Some biodiversity hotspots serve as "evolutionary forewords" that spur fast divergence of tropical plant groupings and the junction of long-distance species distribution, having a significant impact on the establishment and evolution of the world's flora and fauna.

Due to the Hengduan Mountains (HM) region's high northwest and low southeast latitudes, as well as its significant height fluctuations, and its climate, which is characterized by a modest yearly temperature difference and a huge daily temperature difference, a wider range of animal species can survive there (Ren et al., 2020a). As a result, the HM region is listed as one of the 25 worldwide biodiversity hotspots (Li et al., 2014; Qu et al., 2014). Located in the Tibetan Plateau, the HM region is a section of the Qinghai-Tibetan Plateau (QTP). It covers 364,000 square kilometers and is made up of the western Yunnan, northwestern Yunnan, western Sichuan, southeast Tibet, southeast Qinghai, and southwest (Qu et al., 2014). The dramatic topography of the HM region, caused by tectonic uplift during the late Pliocene, resulted in dramatic ecological stratification. As a result, the current HM region is made up of a series of parallel mountains, with elevations ranging from 1000 meters on valley floors to over 5000 meters on mountain peaks (Hwang, 2003). These resemble "sky islands," with deep valleys and "ocesans" of alternate vegetation surrounding them (He and

67 Jiang, 2014). Populations have consequently gotten separated from one another and evolved
68 independently. These "sky islands" mimic an archipelago of islands and mountain ranges by
69 isolating creatures into separate subregions and mountain chains (Zhang, 2012; Li et al.,
70 2014).

71 The refugia theory is one well-known explanation for the high biodiversity (Zhang, 2002;
72 He et al., 2016). Throughout Quaternary ice-age cycles, the HM region in mainland China is
73 regarded as one of the most notable glacial refugia (Qiu et al., 2011; Li et al., 2021). In times
74 of unfavorable climatic circumstances, the complex and diverse ecosystem in the HM region
75 allows for species to move up and down the mountains in search of suitable habitats, reducing
76 the risk of extinction. According to intraspecific phylogeographic studies among species,
77 large valleys functioned as physical barriers for smaller terrestrial animals, and the HM
78 region featured a number of refugia where populations were able to escape the Pleistocene
79 glaciations (He and Jiang, 2014). Another model hypothesizes that the intricate "sky island"
80 split the ecosystems in the highlands, isolating populations of certain species, which led to
81 allopatric speciation (He and Jiang, 2014; He et al., 2016). However, the reasons for this
82 particular diversity are not well understood.

83 Animals display a variety of phenotypic alterations as a result of selection forces acting
84 on heritable features as a result of geographical and temporal heterogeneity (Leinonen et al.,
85 2008). Animals may go through these phenotypic changes to better fit their environment at
86 the physiological, behavioral, and especially morphological levels. Although phenotypic
87 plasticity has been extensively studied and its significance in adaptation and evolution has
88 been well-discussed, the basic driving mechanisms are still unknown (Kelly et al., 2012;

89 Sommer, 2020).

90 Comparative analyses of quantitative genetic and neutral marker differentiation have
91 given researchers a way to assess the relative contributions of stochastic genetic drift and
92 natural selection to the explanation of among-population divergence (Leinonen et al., 2008).
93 In several species, the comparison of quantitative trait across populations (Q_{ST}) and
94 differentiation at neutral molecular markers (F_{ST}), commonly referred to as the Q_{ST}-F_{ST}
95 comparison, revealed that natural selection played a significant role in the cause of
96 differentiation in quantitative traits. In several cases, putative F_{ST} and Q_{ST} differentiation in
97 various populations is compared in order to evaluate their evolutionary signatures and
98 discover potential features implicated in local adaptation.

99 However, raising animals from various populations in a common environment is
100 typically required for estimating the additive genetic variances needed for Q_{ST} (Leinonen et
101 al., 2008; Brommer et al., 2011). As a result, for some wild species, particularly endangered
102 species, the breeding test for estimating the Q_{ST} becomes impractical. Currently, most species
103 substitute quantitative trait analysis (Q_{ST}) with phenotypic divergence in a trait (P_{ST}), and P_{ST}
104 counts are based on phenotypic assessments of a wild trait of several individuals across
105 numerous populations (Brommer et al., 2011). P_{ST}-F_{ST} comparisons, on the other hand, rely
106 on the unrealistic presumption that nonadditive genetic effects and environmental effects may
107 be reduced and that phenotypic variation equals additive genetic variance (Wójcik et al.,
108 2006).

109 *Eothenomys* of subfamily Arvicolinae, which belong to the family Cricetidae in Rodentia,
110 is wildly distributed throughout the Holarctic realm and parts of the Oriental realm (Luo et al.,

111 2004). Long-standing controversy surrounds the precise phylogenetic position of *Eothenomys*.
112 Recently, according to research on the species of *Eothenomys* utilizing molecular and
113 morphological evidence revealed that *Eothenomys* has three subgenera, which includes
114 *Eothenomys*, *Anteliomys*, and *Ermites*. *Eothenomys* consists of *Eothenomys colurnus*,
115 *Eothenomys melanogaster*, *Eothenomys eleusis*, *Eothenomys miletus*, *Eothenomys cachinus*,
116 *Eothenomys fidelis,* and *Eothenomys shimianensis. Anteliomys* consists of *Eothenomys*
117 *chinensis*, *Eothenomys custos*, *Eothenomys olitor*, *Eothenomys proditor*, and *Eothenomys*
118 *wardi. Ermites* is the newly distinguished subgenus, which includes five species, *Eothenomys*
119 *hintoni*, *Eothenomys tarquinius*, *Eothenomys jinyangensis*, *Eothenomys meiguensis*, and
120 *Eothenomys luojishanensis*, respectively (Liu et al., 2012; Zeng et al., 2013).

121 *E. miletus* is a naturally occurring species in Hengduan mountain region (Zhu et al.,
122 2010； Ren et al., 2020b), and is listed in International Union for Conservation of Nature
123 (IUCN). *E. miletus* is one of the representative species for studying the evolution of
124 biodiversity in HM region (Zhu et al., 2008). Despite the numerous of population studies that
125 looked at their distribution, phenotypic morphology (Zhu et al., 2008, 2010, 2011, 2014, 2017;
126 Ren et al., 2020b), and microsatellites (Zhu et al., 2013), our understanding of evolution and
127 adaptation within *E. miletus* populations is limited due to the lack of genomic studies. The
128 primary objective of this paper, we use simple genome sequencing and resequencing to
129 explore the genetic variations and genetic structure among five *E. miletus* populations from
130 HM region, as well as compare the quantitation of the P_{ST} based on the collected the
131 morphological data with F_{ST} estimated using sequencing to assess the relative roles of natural
132 selection. Finally, we provide literature for the similar studies on other wild small mammals

133 from HM region.

134 **MATERIALS AND METHODS**

135 ***Subjects and experimental design***

136 From November 2018 to January 2019, the voles (*Eothenomys miletus*) used in this study
137 were caught in five sites with gradually varying altitudes: Deqin (DQ, n=33); Xianggelila
138 (XGLL, n=33); Lijiang (LJ, n=34); Jianchuan (JC, n=33); and Ailaoshan (ALS, n=33). Figure
139 1A and Table 1 contain comprehensive sampling data. The study's latitude, elevation, and
140 annual mean temperatures came from regional weather services. The livers of animals that
141 were caught in the wild were immediately dissected and frozen in liquid nitrogen after they
142 were weighted and anesthetized. Samples were transported to the Yunnan Normal University
143 lab in dry ice and maintained there in a refrigerator at a temperature of 80℃ until they were
144 analyzed. Using the phenol/chloroform method, the total genomic DNA of the animals was
145 extracted from tissue samples. With the Covaris system, 1-3 g of DNA from each person were
146 cut up into fragments of 200-500 bp (Gene Company, Ltd., Hong Kong, China). The
147 Institutional Animal Care and Use Committee granted its approval to all experimental
148 methods.

149 ***Morphometrics***

150 We created small mammal skull specimens using the Tenebrio molitor larval method.
151 The analysis of the fractured skull specimens was not carried out. At Yunnan Normal
152 University's animal specimens room, 112 complete skull specimens were kept (Kunming,
153 China). Vernier calipers were used to measure external and cranial morphometrics to the
154 nearest 0.01 cm. For each specimen, twenty-one cranial and external characteristics were

155 mentioned. Nine external measurements, including body length (BL), tail length (T1L), torso
156 length (T2L), chest width (CW), chest depth (CD), ear length (EL), ear width (EW), fore limb
157 length (FLL), and hind limb length (HLL), were taken from specimen tags referring to Gao
158 (2017). Twelve cranial measurements were made after Yang (2005) and Xia's measurements
159 (2006). The measurements of the cranium included cranial length (CL), cranial basal length
160 (CBL), cranial height (CH), pillow nose length (PNL), zygomatic breadth (ZB),
161 neurocranium width (NW), covering cap length (CCL), interorbital breadth (IB), eye socket
162 length (ESL), auditory vesicle length (AVL), upper tooth row length (UTRL), and lower tooth
163 row length (LTRL). In order to maximize the sample size, combining males and females for
164 morphological analysis works well because their sexual dimorphism does not differ from
165 groups (Zhang et al, 2019).

166 ***Sample sequencing, read mapping and quality control.***

167 161 voles were utilized in this investigation to produce 464-494 mid-depth specific
168 site-specific amplification fragments (SLAF) of 464-494 insertion lengths using the Rsal
169 enzyme from Beijing Baimai Technology Co., Ltd. (Sun et al., 2013). In SLAF labeling, the
170 target fragment is identified for processing after PCR amplification, purification, mixing, and
171 enzyme digestion (Kozich et al., 2013). A is added at the 3' end to connect the connectors of
172 the double-labeled sequences. Using the Illumina HiSeq 2500 platform, we processed and
173 sequenced the fragments that we had identified. The raw readings were initially filtered using
174 the following criteria: reads that had more than 10% of unidentified nucleotides (N) and more
175 than 50% of low-quality bases (phred quality 5) were both excluded. Then, using the "MEM"
176 approach of Burrows-Wheeler Aligner (BWA 0.7.12-r1039) (Li and Durbin, 2009), and the

177 clean reads were mapped to the reference genome of Prairie voles (*Microtus ochrogaster*)
178 (https://www.ncbi.nlm.nih.gov/genome/10848) (Fan et al., 2019).

179 A 42-degree depth of coverage was repeated with one vole at each point. The BGI
180 platform was then used to process and sequence DNA fragments. Following that, raw reads
181 were first filtered employing Beijing Genomics Institution Co. LTD's SOAPnuke 1.5.6
182 software. Clean reads were then mapped to the Microtus ochrogaster reference genome using
183 the "MEM" algorithm of BWA 0.7.12-r1039 software with the option "-t 8 -k 19 -M -R" (Fan
184 et al., 2019). The SortSam.jar methodology of Picard 1.117 and the RealignerTargetCreator
185 and IndelRealigner tools of GATK 3.3.0 were used, respectively, to sort and correct the final
186 BAM files used in the subsequent analysis (McKenna et al., 2010).

187 ***SNP Calling and Filtering***

188 In order to estimate the sequencing quality value Q, the reads considered to be of low
189 quality were those with joint and 50% bases with a Q10 value. Q = -10*log10e. From the
190 straightforward genome sequencing of 161 voles, we obtained the SNPs using the innovative
191 technology SLAF-seq (Beijing Baimai Biotechnology Co. LTD). Using the call function in
192 Bcftools 1.10, we called variants after using SAMtools 1.2 to gather summary data from
193 BAM files and calculate the likelihood of potential genotypes (Li et al. 2009). Segments of
194 the reference genome were separated and examined simultaneously. Segments of the
195 reference genome were separated and subjected to parallel analysis. The raw SNPs were then
196 filtered using a customized script using the following criteria to obtain high-quality variants:
197 Completeness > 0.5 and minimal allele frequency > 0.05 are the criteria.

198 Clean paired-end reads from individuals were aligned to the resequenced assembled vole

199 reference genome using BWA 0.7.12-r1039. Then, SNPs were identified using GATK 3.3.0,
200 and the clean SNPs were aligned using GATA 3.3.0 hard filter with the following filter
201 parameters: QD 2.0, FS > 60.0, MQ 40.0, ReadPosRankSum -8.0, and MQRankSum -12.5.
202 Only SNPs with high second-order credibility were retained for further analysis after the
203 SNPs were filtered by minimum allele frequency (MAF) = 0.06 and maximum missing rate =
204 25%.

205 ***Population structure***

206 Population structure analysis was done using the ADMIXTURE 1.3.0 (Alexander et al.,
207 2009), which calculates individual ancestry and admixture ratios based on K ancestral
208 populations. We examined the number of genetic clusters (K) ranging from one to 10 while
209 running ADMIXTURE five times to gauge convergence (Alexande et al., 2009). Additionally,
210 we performed a cross-validation test with frappe to determine the best match K value (Tang
211 et al., 2005). Using EIGENSOFT 3.0 software, principal component analysis (PCA) was
212 carried out (Patterson et al., 2006). The neighbor-joining (NJ) approach in MAGA 7.0.26 was
213 employed to reconstruct phylogenetic trees of 161 individuals (Koichiro et al., 2011; Ren et
214 al., 2022).

215 ***Genetic Diversity***

216 The expected heterozygosity (He) and observed heterozygosity (Ho) were calculated
217 using PLINK 1.9 (Purcell et al., 2007) to test the genetic diversity indices of five populations
218 based on high-consistency SNPs, and the, observed allele number, expected allele number,
219 Nei diversity index, and polymorphy information content (PIC) were calculated using a
220 customized Perl script. We used SPSS 26.0) to calculate Pearson's correlation coefficient (r^2)

221 between each pair of variables in order to further quantify the impact of environmental
222 variables, such as altitude, temperature, and latitude, on genetic diversity at five geographic
223 populations (Qu et al., 2014).

224 ***Demographic history reconstruction and gene flow***

225 The maximum likelihood method and a Bayesian statistical model were employed in Perl
226 to estimate pairwise relative migration rates and direction based on the retroactive theory
227 (Beijing Baimai Biotechnology Co. LTD) (Sundqvist et al., 2016; Schiffels and Durbin,
228 2014). The Bayesian statistical model of MIGRATE-N software was used to estimate
229 pairwise relative migration rates and directionality between populations based on the ancestor
230 tracing theory. Additionally, five populations' gene flow was examined using the TREEMIX
231 software. The miss rate is 0.8 at its highest. R becomes 0.6 after the chain-unbalanced SNP is
232 instantly removed. Additionally, the pairwise sequentially Markovian coalescent (PSMC)
233 model, which has been extensively used in other mammals, was used to estimate changes in
234 effective population size based on heterozygous sites across the genome. In this study, the
235 generation time and the mutation rate were separately set at 0.5 years and 2.96×10^{-9} (Teng et
236 al., 2017). The remaining high-credibility SNPs from genome resequencing were used for
237 PSMC analysis after SNPs with a minimum allele frequency of 0.06 and a maximum missing
238 rate of 25% were filtered.

239 ***Neutral genetic differentiation and phenotypic differentiation***

240 SNPRelate package in R 3.6.3 was used to calculate pairwise F_{ST} (Zheng et al., 2012),
241 and Prism 9 was used to build a heat map of the pairwise F_{ST} value. Based on Pearson's
242 product-moment correlation, the Mantel test of matrix correspondence (Mantel, 1967) was

243 applied to test correlations between geographic distance, environment distance, altitude
244 distance, temperature distance, precipitation distance, pairwise F_{ST}, and $F_{ST}/(1-F_{ST})$ in order
245 to test the effects of geographic distance and environmental differences on genetic
246 differentiation. This was done using the Ecodist package in R 3.6.3 (Rousset, 1997). On
247 topographic maps of the study area, point-to-point geographic distances were calculated
248 (Browne & Ferree, 2007). Moreover, we gathered environmental data from WorldClim 2.0
249 for sampling locations using 19 common bioclimatic variables (Fick & Hijmans 2017).
250 ArcMap 10.2 was used to convert the data. The 19 standard bioclimatic variables that
251 correlate to temperature were utilized as temperature data, while the 19 typical bioclimatic
252 variables that relate to precipitation were used as precipitation data.

253 To calculate the distance in environment, temperature, and precipitation, we employed
254 the Pearson distance measurement method. General linear regression analysis in R 3.6.3 was
255 used to investigate the relationship between geographic distance and environmental distance.
256 The pairwise F_{ST} or $F_{ST}/(1-F_{ST})$ was employed as the response, the geographic distance as the
257 predictor, and the environmental distance as the condition factor to assess isolation by
258 distance (IBD). The geographic distance was utilized as the condition element to investigate
259 isolation by environment (IBE), isolation by temperature (IBT), and isolation by precipitation
260 (IBP). Moreover, the distance in altitude between paired sampling sites was calculated.
261 Finally, we utilized Canoco 5 to perform redundancy analysis (RDA).

262 Using the SPSS 26.0 program, the body mass and twenty-one exterior and cranial
263 character data were evaluated. One-way analysis of variance (ANOVA) and LSD post-hoc
264 tests were used to assess group differences in attributes; $P < 0.05$ was deemed statistically

265 significant, while $P < 0.01$ was deemed extremely significant. Prism 9 was used to perform
266 Highcharts and Boxplot. Using the online Heatmapper, a cluster analysis plot and correlation
267 matrix map between physical characteristics and environmental factors were created.

268 Divergence at phenotypic traits will be greater than that seen for neutral loci under
269 divergent selection. Common garden and reciprocal transplant studies are not viable for the
270 species since the voles employed in this study are wild populations. P_{ST} measures the
271 percentage of among-population phenotypic variance in quantitative characteristics and is
272 equivalent to Q_{ST} (Spitze, 1993), which quantifies the proportion of among-population
273 genetic variance in quantitative traits:

274 $$P_{ST} = \frac{c\sigma^2{}_B}{c\sigma^2{}_B + 2h^2\sigma^2{}_W}$$ (Raeymaekers et al., 2007)

275 where $\sigma^2{}_B$ is the variance between populations, $\sigma^2{}_W$ is the variance within populations, and h^2
276 the heritability. The scalar c expresses the proportion of the total variance that is presumed to
277 be because of additive genetic effects across populations, assuming that environmental
278 variance among samples is randomly distributed or absent and that heritability (h^2) within
279 samples is 0.5. The consequences of departure from these assumptions are considered below
280 in the Discussion sections. Phenotypic variance components were estimated following Sokal
281 & Rohlf 1995. The pairwise P_{ST} values for individual attributes were compared with the
282 pairwise F_{ST} (P_{ST}/F_{ST} value) to assess the degree of phenotypic divergence with neutral
283 genetic divergence. The two-way clustering heat map of the P_{ST}/F_{ST} value between paired
284 populations was built using the online Heatmapper. We tested correlations between
285 geographic distances, population pairwise altitudinal differences, pairwise F_{ST}, and pairwise
286 P_{ST} using the Mantel test of matrix correspondence (Mantel, 1967) as implemented in the

287 Ecodist package in R 3.6.3. To determine if neutral genetic differentiation accounts for the
288 divergence in quantitative characteristics, a correlation test between pairwise F_{ST} and
289 pairwise P_{ST} was first carried out for each trait. In order to find out whether divergence in
290 quantitative traits was connected to geographic distance and altitudinal differences, a
291 correlation test between pairwise altitudinal differences, geographic distance, and pairwise
292 P_{ST} was run for each variable. Geographic distances between two points were calculated
293 using topographic maps of the study area.

294

295 **RESULT**

296 ***SNP Calling***

297 Five *E. miletus* populations from the Hengduan mountain regions were sampled by us,
298 totaling 161 individuals (Figure 1A, and Table 1). 363.16 million pair-end reads with an
299 average of 92.23% Q30 and 42.09% GC were produced after quality control (Supplementary
300 table 1). 161 individuals had a total of 847,420 SLAF labels, including 470,440
301 polymorphism labels, which were gathered (Supplementary table 2). After quality control, we
302 successfully identified 2,221,486 SNPs from 161 voles (Supplementary table 3). Additionally,
303 we obtained 0.645 Tb of clean data with average Q20 and Q30 values of 97.72% and 92.85%,
304 respectively, by sequencing at a depth coverage of 38.36, and 108,005,364 SNPs were
305 gathered by comparing with the first 40 chromosomes of the reference genome
306 (Supplementary figure 1 and table 5).

307 ***Population Structure***

308 Five populations of voles could be distinguished using mixture analyses based on the

309 same SNPs and assuming various numbers of ancestry components (K) (Figure 1B).
310 Population structure was evident, with K = 4 providing the strongest statistical evidence. First,
311 at K = 1, the five populations of mice united to form one ancestor. The ALS group displayed
312 unique ancestries from other populations when K = 2. Additionally, with K = 3, the JC
313 population was further distinguished from the other populations. This is consistent with the
314 PCA results, which distinguished the JC population from the ALS population using the first
315 and second main components (PC1 and PC2). Moreover, with K = 4, a portion of the XGLL
316 individuals and the JC population formed one ancestra, and the remainder XGLL individuals
317 and the DQ population formed one ancestra, in accordance with PCA, which further divided
318 the LJ population and the DQ population (Figure 1C and Supplementary Figure 2). The five
319 groups spread over these locations showed varying degrees of mixed ancestry as K climbed
320 from 5 to 10. The line chart in Figure 1B displays cross-validation errors for various K values,
321 with K = 4 having the lowest cross-validation error rate.

322 Following that, we used phylogenetic reconstruction to categorize the individuals (Figure
323 1D). The clustering of populations, which showed four clusters, revealed that the ALS and JC
324 populations each formed one cluster, while a portion of the XGLL population with DQ
325 individuals formed one cluster and the remaining XGLL population with LJ individuals
326 formed another. This is in line with what our structure analysis and PCA revealed.

327 ***Genetic Diversity***

328 Table 2 contains a summary of the various population genetic diversity indicators, such
329 as the nucleotide polymorphism (θπ), Tajima D, observed allele number, expected allele
330 number, observed heterozygous (Ho), expected heterozygous (He), Nei diversity index,

331 Shanon wiener index, as well as polymorphysm information content (PIC). The genetic
332 diversity of the five *E. miletus* populations from the Hengduan mountain regions was highest
333 in the ALS population, followed by JC population, and least in the XGLL population.

334 The impact of environmental factors on genetic diversity was then further investigated
335 using general linear analysis and multiple linear regression analysis, as shown in Table 1.
336 Some intriguing links have been found. With the exception of Tajima, D, and observed
337 heterozygotes, there was no link between altitude and genetic diversity indices ($P > 0.05$),
338 however there were substantial relationships between ambient temperature, latitude, and
339 indexes ($P < 0.05$).

340 ***Demographic history and gene flow***

341 To estimate the pairwise relative migration rates and direction between pairwise
342 populations, we employed the Migrate-N. (Figure 2A). Although average migration rates
343 across all groups were more than one migrant per generation, there were asymmetric gene
344 flow (*Nm*) patterns. According to the F_{ST} technique, there were 0 to 62.52 migrants on
345 average per generation between all populations. There were asymmetric patterns of gene flow
346 between the DQ and XGLL populations and the XGLL and LJ populations, with the Nm
347 between the DQ and XGLL populations having the highest mean of 62.92. The next Nm was
348 from the XGLL population to the LJ population. Furthermore, there were no Nm between the
349 JC and ALS populations as well as the LJ and JC populations. Additionally, the maximum
350 likelihood tree of *Nm* between five populations was constructed using Treemix
351 (Supplementary Figure 3); the outcome closely matched the finding from our Migrate-N
352 result.

353 Changes of the effective population size (Ne) over time were evaluated with the PSMC
354 model for each five populations (Figure 3B), and showed a similar pattern. There were
355 variety phases of Ne, and the variations in Ne aligned well with the changes in historical
356 world temperature. First, Ne began to increase during Quaternary glaciation (2000~3000Kya,
357 Ehlers and Gibbard, 2008) until Marine Isotope Stage 12 (500Ka ± 5Ka BP. (Howard, 1997).
358 Second, there were two population bottleneck effect which happened about 500 Ka and 30Ka
359 years ago, the two period of low temperature in history (Howard, 1997).
360 Third, the second increasing time of the Ne during Marine Isotope Stage 5 (MIS5,
361 130Ka-80Ka BP. Lisiecki and Raymo, 2005), the last major interglacial stage in history, and
362 reach a higher level during Marine Isotope Stage 3 (MIS3, 60Ka-25Ka BP. Siddall et al.,
363 2008), a special period in the last glacial period which has the extremely unstable climatic
364 conditions and many climatic abrupt events, while the Ne begin to decrease during the colder
365 substage MIS3c (39.3Ka-26.5Ka BP. Wulf et al. 2018) until the end of the last glacial period
366 (11.5Ka BP. Blunier, 2001). After the periods of fluctuation, the Ne decreased.
367 ***Neural genetic differentiation and phenotypic differentiation***
368 The pairwise fixation (F_{ST}) ranged from 0.019 to 0.188 (average, 0.124) in this study.
369 Moreover, the heat map of the pairwise F_{ST} showed that JC population and ALS population
370 have high genetic differentiation with the other three populations, and there were medium
371 score genetic differentiation between the remainder populations (Figure 3A). In addition,
372 there was the largest values generally pairwise F_{ST} between ALS population and JC
373 population as well as the lowest pairwise F_{ST} between DQ population and XGLL population.
374 Mantel tests for groups revealed a strong relationship between pairwise F_{ST} and $F_{ST}/(1-F_{ST})$

375 as well as temperature distance (IBT) (mantel r_{FST}= 0.741; P_{FST} < 0.05; mantel $r_{FST/(1-FST)}$=
376 0.766; $P_{FST/(1-FST)}$ < 0.01, Figure 3D, E), while the other distances, including geographic
377 distances (IBD) (mantel r_{FST}= 0.618; P_{FST} > 0.05; mantel $r_{FST/(1-FST)}$= 0.627; $P_{FST/(1-FST)}$ > 0.05,
378 Figure 3B, C), altitude distance (IBA) (mantel r_{FST}= 0.182; P_{FST}> 0.05; mantel $r_{FST/(1-FST)}$=
379 0.166; $P_{FST/(1-FST)}$ > 0.05, Figure 3F, G), climate distance (IBC) (mantel r_{Fst}= -0.528; P_{FST}>
380 0.05; mantel $r_{Fst/(1-FST)}$= -0.520; $P_{FST/(1-FST)}$ > 0.05, Figure 3H, I), precipitation distance (IBP)
381 (mantel r_{FST}= -0.443; P_{FST} > 0.05; mantel $r_{FST/(1-FST)}$= -0.442; $P_{FST/(1FST)}$ > 0.05, Figure 3J, K),
382 had no significant correlation with pairwise F_{ST} and $F_{ST}/(1-F_{ST})$. Moreover, RDA analysis
383 showed that there was a highest contribution of temperature distance on genetic diversity
384 (Figure 3L).

385 There were extremely significant differences in body mass as well as twenty external
386 and cranial characters, expect AVL, between five populations (P < 0.01) (Figure 4 A, B). The
387 body mass and size of LJ population, JC population and ALS population were greater than
388 DQ population and XGLL population. Moreover, The results of single cluster analysis
389 revealed that revealed the grouping of populations, which showed two clusters, DQ
390 population and XGLL population formed one cluster, and JC population, LJ population and
391 ALS population formed one clusters (Figure 4C). Finally, there were significant correlations
392 between most phenotypic traits and environment factors, which had positive correlation with
393 annual environment temperature, and had negative relationship with altitude and latitude (P <
394 0.05) (Figure 4 D).

395 We further calculated the pairwise P_{ST} of all phenotypic traits between five populations,
396 and compared with the pairwise F_{ST}. First the results of violin diagram show that the

397 probability of P_{ST} more than F_{ST} is large (Figure 5 A). Moreover, the results of independent
398 sample t test showed that P_{ST} of all tested traits was significantly greater than F_{ST} ($P < 0.01$).
399 From the two-way clustering heat map of P_{ST}/F_{ST} value, several interesting findings have
400 emerged. First, most of pairwise P_{ST} of phenotypic traits were higher than the pairwise F_{ST}
401 (Figure 5 B, Supplement table 6). Moreover, the P_{ST}/F_{ST} value differed significantly, and
402 there was the highest P_{ST}/F_{ST} value between DQ population and XGLL population than the
403 other pairwise population, followed by the ratio of between XGLL population and LJ
404 population.

405 Mantel tests showed no relationship between pairwise P_{ST} and F_{ST} for most traits (Table
406 3), but the pairwise P_{ST} for BM, EL, CL, CBL and AVL in *E. miletus* were significantly
407 correlated with population pairwise F_{ST}. Mantel tests showed a significant correlation
408 between pairwise P_{ST} for BM, BL, T_1L, CW, FLL, HLL, IB and UTRL in *E. miletus* and
409 population altitudinal differences, however, there were no significant correlation between
410 pairwise P_{ST} for traits except for the ZB in *E. miletus* and population geographic distance
411 (Table 3).

412

413 **DISCUSSION**

414 Phenotypic changes at the morphological, physiological and behavioral levels to adapt
415 the diverse environment in HM region were found in *E. miletus* (Zhu et al., 2014; Zhang et al.,
416 2019; Ren et al., 2020b). Genetic variations were also found in five *E. miletus* populations
417 from HM region in this study, and although sharing a similar demographic history, the
418 populations had a clear genetic structure. According to the result of population structure,

419 there were four clusters in genetic level, which grouped together a part of XGLL individuals
420 and JC population, and the remainder of XGLL individuals and DQ population, and JC
421 population as well as ALS population respectively formed a single cluster. This is different
422 from the statistic of phenotypic variations, which clustered together the DQ population and
423 XGLL population, and grouped together the LJ population, JC population and ALS
424 population (Zhang et al., 2019; Ren et al., 2020a).

425 High genetic variation can serve as the basis for adaptability to environmental change
426 through natural selection, which is essential to the long-term survival of populations
427 (Ellegren et al., 2016; Bijak et al., 2018), as seen in this study with *E. miletus*. Geographical
428 differences result in populations displaying varying degrees of genetic diversity (Ellegren et
429 al., 2016). The study is selected populations ascend in altitude order. LJ population, JC
430 population and ALS population belong to a relative low altitude with range from 2000m to
431 3000m, as well as XGLL population and DQ population belong to a relative high altitude
432 which over 3000m. The annual average temperature of the environment is counter with the
433 altitude. Our data show that the relative low altitude populations had higher genetic diversity
434 than the relative high altitude populations, but there were no correlation between genetic
435 diversity indexes and altitude. The reason may attribute to the altitude selected in the present
436 study, as the altitude of five population over 2000m reached a high altitude level.
437 Nevertheless, most of genetic diversity indexes had significant correlation with annual
438 average temperature and latitude in this study, indicating that annual average temperature and
439 latitude may play important roles in the genetic diversity of *E. miletus*, while, whether the
440 other factors, such as food, gut microbiota and so on, can play a role in genetic diversity

441 remains to be explored.

442 It is interesting to note that there were asymmetric gene flow patterns in five *E. miletus*
443 populations. First, there was relative high gene flow between DQ population and XGLL
444 population as well as between XGLL population and LJ population, and these better proves
445 the population structure of *E. miletus* in this study, which clustered together respectively. In
446 addition, JC population and ALS population had low gene flow with the other populations,
447 and there was even no gene flow between LJ population as well as ALS population and JC
448 population. This result is consist with that the JC population and ALS population form a
449 cluster respectively. These data may indicate that five *E. miletus* populations exhibit a
450 isolation-by-island model. This contrasts with the isolation-by-distance concept that is
451 present in red-backed vole in southern Virginia (Reese et al., 2001) and southern Appalachia
452 (Browne and Ferree, 2007). The isolation-by-island model predicts that there is no
453 relationship between the distance separating populations and the amount gene flow, in
454 contrast to the isolation-by-distance mode, which asserts that populations separated by shorter
455 distances will experience higher rates of gene flow than populations separated by longer
456 distances (Browne and Ferree, 2007). Isolation-by-island concept typically manifests in
457 animals whose habitat is cut off by an extreme environment, and in those species, the
458 distributions of the sub-populations are typically entirely discontinuous in that environment
459 (Qu et al., 2004). These findings show that barriers to gene flow among *E. miletus*
460 populations existed as a result of the extreme topography of the HM region caused by the
461 geological uplift that occurred during the late Pliocene.

462 It seems conceivable that relatively stable habitats appropriate in the HM region, known

463 as refugia, emerge after the fast uplift of the HM region towards the end of the Pliocene for *E.*
464 *miletus* population to survive extreme climate in Quaternary glaciation (Qu et al., 2014; He et
465 al., 2016; Zhou et al., 2006). Moreover, most probably *E. miletus* populations were pushed up
466 and down the hillsides in response to the varying extent of glaciers during the Pleistocene,
467 causing populations interflow increase. Thus, there was a increase in Ne during the begging
468 of Quaternary glaciation. While, climate fluctuations strongly affected the Ne of the species
469 after the formation of geographical isolation in HM region, as the effective population size
470 historically decreased during cold periods, especially during the last ice age.

471 There was medium or high score genetic differentiation between five *E. miletus*
472 populations, and Mantel test between pairwise F_{ST} and geographic also support the
473 isolation-by-island model, which showed that there was no correlation between pairwise F_{ST}
474 and geographic distance in the present study (Browne and Ferree, 2007). Phenotypic changes
475 at the morphological levels to adapt the diverse environment in HM region were also found in
476 *E. miletus* in this study. This is consist with the previous studies (Zhang et al., 2019; Ren et
477 al., 2020a). Moreover, morphological changes had negative correlation with altitude and
478 latitude, and positive correlation with annual environment temperature, indicating that
479 morphological traits of *E. miletus* dose not obey the Bergmann's rule (Bergmann, 1847;
480 Ashton et al., 2000).

481 No data were available to estimate the genetic variances of traits in this study due to the
482 fact that the animals in this study are wild, but we can determine the effect on P_{ST} under
483 different h^2 conditions. We further calculated the P_{ST} value using four different heritability
484 estimates (0.25, 0.5, 0.75, and 1), based on the assumption that there is no environmental

variance. The graphs in Figure 6 showed the value that the P_{ST}-F_{ST} ratio would take for different values of h^2. The majority of P_{ST} values were greater than pairwise the F_{ST} value, even though the pairwise F_{ST} value was at its minimum when the h^2 was assumed to be one. However, it is well understood that the h^2 can not be one, and must be less than one. With our original assumptions, we concluded that most traits are the consequence of natural selection. Except for a few exceptions, the only conditions under which P_{ST} would be much lower than F_{ST} are if environmental variance is close to zero, and the critical value of c when the h^2 is one is shown in Supplement table 7. These conditions are unlikely to be compatible in nature because nonheritable variance should be environmentally pliable (Wójcik et al., 2006).

CONCLUSION

In this study, we investigated the widely dispersed *E. miletus* in the HM region and used population genomic techniques to provide insights on its differentiation, adaptation, and history. In conclusion, our data show that *E. miletus* from the HM region exhibits phenotypic and genetic alterations related to naturally occurring diverse environments. It's interesting to note that there are two phenotypic clusters and various phenotypic and genetic change patterns. Furthermore, phenotypic and genetic changes are linked to environmental factors, such as latitude, altitude, and average annual temperature, and phenotypic traits are more influenced by environmental factors; however, it is still unknown whether other environmental factors may also have an impact on phenotypic and genetic changes. Additionally, the significant biological stratification brought on by the tectonic uplift of the HM region during the late Pliocene results in spectacular topography, which has an impact on

507 the asymmetric gene flow patterns found in *E. miletus*. Five *E. miletus* populations
508 demonstrate an isolation-by-island model, which is supported by gene flow and a link
509 between FST and geographic distance. Last but not least, PST estimates for the majority of
510 wild traits are higher than differentiation at neutral molecular markers, indicating that
511 directional natural selection favoring various phenotypes in various populations was likely
512 involved in achieving thus much divergence. Our findings provide as a foundation for studies
513 on other HM region wild small animals.

514 **SUPPLEMENTARY DATA**

515 Supplementary data to this article can be found online.

516 **COMPETING INTERESTS**

517 The authors declare no competing financial interests.

518 **ACKNOWLEDGEMENTS**

519 We appreciate the assistance of all the Physiological Ecology Group members at Yunnan
520 Normal University in carrying out the experiments and discussing the findings. The Yunnan
521 Ten Thousand Talents Plan Young & Elite Talents Project (YNWR-QNRC-2019-047),
522 National Natural Scientific Foundation of China (Grant No. 32160254), National Natural
523 Scientific Foundation of China (Grant No. 31760118), and the Yunnan Provincial
524 Middle-Young Academic and Technical Leader (2019HB013) candidate provided financial
525 support for this work.

526 **REFERENCE**

527 Alcala N, Goudet J, Vuilleumier S. 2014. On the transition of genetic differentiation from
528 isolation to panmixia: What we can learn from Gst and D. *Theoretical population*

biology, **93**: 75–84.

Alexander DH, Novembre J, Lange K. 2009. Fast model-based estimation of ancestry in unrelated individuals. *Genome Research*, **19**: 1655–1664.

Alho JS, Herczeg G, Söderman F, Laurila A, Jönsson KI, Merilä J. 2010. Increasing melanism along a latitudinal gradient in a widespread amphibian: local adaptation, ontogenic or environmental plasticity? *BMC Evolutionary Biology*, **10**: 317.

Ashton KG, Tracy MC, Queiroz A. 2000. Is Bergmann's rule valid for mammals?. *American Naturalist*, **156**(4): 390–415.

Bergmann C. 1847. Ueber die Verhältnisse der Wärmeökonomie der Thiere zu ihrer Grösse. *Goettinger Studien*, **3**: 595–708.

Bijak AL, Dijk KJ, Waycott M. 2018. Population structure and gene flow of the tropical seagrass, *Syringodium filiforme*, in the Florida Keys and subtropical Atlantic region. *PLoS One*, **13**(9): e0203644.

Blunier T. 2001. Timing of millennial-scale climate change in Antarctica and Greenland during the last glacial period. *Science*, **291**(5501): 109–112.

Brommer JE. 2011. Whither P_{ST}? The approximation of Q_{ST} by P_{ST} in evolutionary and conservation biology. *Journal of Evolution Biology*, **24** (6): 1160–1168.

Browne RA, Ferree PM. 2007. Genetic structure of Southern Appalachian "Sky Island" populations of the Southern Red-Backed Vole (*Myodes gapperi*). *Journal of Mammalogy*, **88**(3): 759–768.

Ehlers J, Gibbard P. 2008. Extent and chronology of quaternary glaciation. *Congress of the International-union-for-quaternary-research*, **31**(2): 211–218.

551 Ellegren H, Galtier N. 2016. Determinants of genetic diversity. *Nature Review Genetics*,
552 **17**(7): 422–433.
553 Fan Y, Ye MS, Zhang JY, Xu L. & Yu DD. 2019. Chromosomal level assembly and
554 population sequencing of the Chinese tree shrew genome. *Zoological Research*, **40**:
555 488–505.
556 Fick SE, Hijmans RJ. 2017. WorldClim 2: New1-km spatial resolution climate surfaces for
557 global land areas. *International Journal of Climatology*, **37**: 4302–4315.
558 Gao WR, Zhu WL, Fu JH Yang T, Wang ZK. 2017. Morphometric variation of tree shrews
559 (*Tupaia belangeri*) from different regions. *Animal Biology*, **67**: 177–189.
560 He K, Hu NQ, Chen X, Li JT, Jiang XL. 2016. Interglacial refugia preserved high genetic
561 diversity of the Chinese mole shrew in the mountains of southwest China. *Heredity*,
562 **116**(1): 23–32.
563 He K., Jiang X. 2014. Sky islands of southwest China. I: An overview of phylogeographic
564 patterns. *Chinese Science Bulletin*, **59**(7): 585–597.
565 Howard WR. 1997. Palaeoclimatology–A warm future in the past. *Nature*, **388**(6641):
566 418–419.
567 Hutchison DW, Templeton AR. 1999. Correlation of pairwise genetic and geographic distance
568 measures: inferring the relative influences of gene flow and drift on the distribution of
569 genetic variability. *Evolution*, **53**(6): 1898–1914.
570 Hwang SY, Lin TP, Ma CS, Lin CL, Chung JD, Yang JC. 2003. Postglacial population growth
571 of *Cunninghamia konishii* (Cupressaceae) inferred from phylogeographical and
572 mismatch analysis of chloroplast DNA variation. *Molecular Ecology*, **12**(10):

573 2689–2695.

574 Kelly SA, Panhuis TM, Stoehr AM. 2012. Phenotypic plasticity: molecular mechanisms and
575 adaptive significance. *Comprehensive Physiology*, **2**(2): 1417–1439.

576 Koichiro T, Daniel P, Glen S, Masatoshi N, Sudhir K. 2011. MEGA5: Molecular evolutionary
577 genetics analysis using maximum likelihood, evolutionary distance, and maximum
578 parsimony methods. *Molecular Biology and Evolution*, **28**(10): 2731–2739.

579 Kozich JJ, Westcott SL, Baxter NT, Highlander SK, Schloss PD. 2013. Development of a
580 dual-index sequencing strategy and curation pipeline for analyzing amplicon sequence
581 data on the MiSeqIllumina sequencing platform. *Applied and environmental*
582 *microbiology*, **79**(17): 5112–5120.

583 Lehtonen PK, Laaksonen T, Artemyev AV, Belskii E, Both C, Bures S, et al. 2009.
584 Geographic patterns of genetic differentiation and plumage colour variation are different
585 in the pied flycatcher (*Ficedula hypoleuca*). *Molecular Ecology*, **18**(21): 4463–4476.

586 Leinonen T, Cano JM, Makinen H, Merila J. 2006. Contrasting patterns of body shape and
587 neutral genetic divergence in marine and lake populations of threespine sticklebacks.
588 *Journal Evolution Biology*, **19**(6): 1803–1812.

589 Leinonen T, O'Hara RB, Cano JM, & Merilä J. 2008. Comparative studies of quantitative trait
590 and neutral marker divergence: a meta-analysis. *Journal of Evolution Biology*, **21**(1):
591 1–17.

592 Li H, & Durbin R. 2009. Fast and accurate short read alignment with Burrows–Wheeler
593 transform. *Bioinformatics*, **25**(14): 1754–1760.

594 Li H., Handsaker B, Wysoker A, Fennell T, Ruan J, Homer N, et al. 2009. The sequence

alignment/map format and SAMtools. *Bioinformatics*, **25**(16): 2078–2079.

Li A, Hou Z. 2021. Phylogeographic analyses of poplar revealed potential glacial refugia and allopatric divergence in southwest China. *Mitochondrial DNA Part A: DNA Mapping Sequence, and Analysis*, **32**(2): 66–72.

Li XH, Zhu XX, Niu Y, & Sun H. 2014. Phylogenetic clustering and overdispersion for alpine plants along elevational gradient in the Hengduan Mountains Region, southwest China. *Journal of Systematics and Evolution*, **52** (3): 280–288.

Liu SY, Liu Y, Guo F, Sun ZY, Murphy RW, Fan ZX, Fu JR, Zhang YP. 2012. Phylogeny of Oriental voles (Rodentia: Muridae: Arvicolinae): molecular and morphological evidence. Zoological Science, **29**: 610–622.

Lisiecki LE, Raymo ME. 2005. A Pliocene-Pleistocene stack of 57 globally distributed benthic δ18O records. *Paleoceanography*, **20**(1): PA1003.

Luo J, Yang DM, Suzuki H, Wang YX, Chen WJ, Campbell KL, et al. 2004. Molecular phylogeny and biogeography of Oriental voles: genus *Eothenomys* (Muridae, Mammalia). *Molecular Phylogentics and Evolution*, **33**(2): 349–362.

Mantel N. 1967. The detection of disease clustering and a generalized regression approach. *Cancer Research*, **27**(2): 209–220.

Marin S, Gibert A, Archambeau J, Bonhomme V, Lascoste M, Pujo B. 2020. Potential adaptive divergence between subspecies and populations of snapdragon plants inferred from Q_{ST}-F_{ST} comparisons. *Molecular Ecology*, **29**(16): 3010–3021.

Merila¨ J. 1997. Quantitative trait and allozyme divergence in the greenfinch (*Carduelis chloris*, Aves: Fringillidae). *Biological Journal of the Linnean Society*, **61**: 243–266.

617 Merilä J, & Crnokrak P. 2001. Comparison of genetic differentiation at marker loci and
618 quantitative traits. *Journal of Evolution Biology*, **14**(6): 892–903.
619 McKenna A, Hanna M, Banks E, Sivachenko A, Cibulskis K, Kernytsky A, et al. 2010. The
620 Genome Analysis Toolkit: a MapReduce framework for analyzing next-generation DNA
621 sequencing data. *Genome research*, **20**(9): 1297–1303.
622 Morgan TJ, Evans MA, Jr TG, Swallow JG, Carter PA. 2005. Molecular and quantitative
623 genetic divergence among populations of house mice with known evolutionary histories.
624 *Heredity*, **94**(5): 518–525.
625 Nei M, Li WH. 1979. Mathematical model for studying genetic variation in terms of
626 restriction endonucleases. *Proceedings of the National Academy of Sciences of the*
627 *United States of America*, **76**(10): 5269–5273.
628 Patterson N, Price AL, Reich D. 2006. Population structure and eigenanalysis. *PLoS Genet*,
629 **2**(12): e190.
630 Purcell S, Neale B, Todd-Brown K, Thomas L, Ferreira MAR, Bender D, et al. 2007. PLINK:
631 a tool set for whole-genome association and population-based linkage analyses.
632 *American Journal of Human Genetics* **81:** 559–575.
633 Qiu YX, Fu CX, Comes HP. 2011. Plant molecular phylogeography in China and adjacent
634 regions: tracing the genetic imprints of Quaternary climate and environmental change in
635 the world's most diverse temperate flora. *Molecular Phylogenetics and Evolution*, **59**(1):
636 225–244.
637 Qu RL, Hou L, Lv LL, Li HY. 2004. The gene flow of population genetic structure. *Hereditas*,
638 **26**(3): 377–382.

Qu YH, Ericson PGP, Quan Q, Song G, Zhang RY, Gao B, et al. 2014. Long-term isolation and stability explain high genetic diversity in the Eastern Himalaya. *Molecular Ecology*, **23**(3): 705–720.

Raeymaekers JAM, Houdt JKJV, Larmuseau MHD, Geldof S, Volckaert FAM. 2007. Divergent selection as revealed by P(ST) and QTL-based F(ST) in three-spined stickleback (*Gasterosteus aculeatus*) populations along a coastal-inland gradient. *Molecular Ecology*, **16**(4): 891–905.

Reese CL, Waters M, Pagela JF, Brown BL. 2001. Genetic structuring of relict populations of Gapper's red-backed vole (*Clethrionomys gapperi*). *Journal of Mammalogy*, **82**(2): 289–301.

Ren Y, Jia T, Zhang D, Zhang H, Wang ZK, Zhu WL. 2020a. Phenotypic diversity of the *Eothenomys miletus* at different areas of Yunnan range in Hengduan mountains. *Journal of Biology*, **37**(6): 79–84.

Ren Y, Liu PF, Zhu WL, Zhang H, Cai JH. 2020b. Higher altitude and lower temperature regulate the body mass and energy metabolism in male *Eothenomys miletus*. *Pakistan Journal of Zoology*, **52**(1): 139–146.

Ren Y, Jia T, Zhang H, Zhu W, Wang Z. 2022. Population genomics provides insights into the evolution and adaptation of tree shrews (*Tupaia belangeri*) in China. *Integrative Zoology*, **00**: 1–18.

Rousset F. 1997. Genetic differentiation and estimation of gene flow from F-statistics under isolation by distance. *Genetics*, **145**: 1219–1228.

Saether SA, Fiske P, Kålås JA, Kuresoo A, Luigujõe L, Piertney SB, et al. 2007. Inferring

661 local adaptation from Q_{ST}-F_{ST} comparisons: neutral genetic and quantitative trait
662 variation in European populations of great snipe. *Journal of Evolutionary Biology*, **20**(4):
663 1563–1576.
664 Siddall M, Rohling EJ, Thompson WG, & Waelbroeck C. 2008. Marine isotope stage 3 sea
665 level fluctuations: data synthesis and new outlook. *Reviews of Geophysics*, **46**(4):
666 RG4003.
667 Sokal RR, Rohlf FJ. 1995. Biometry, 3rd edn. Freeman, New York. pp. 208–217.
668 Sommer RJ. 2020. Phenotypic plasticity: from theory and genetics to current and future
669 challenge. *Genetics*, **215**(1): 1–13.
670 Spitze, K. 1993. Population structure in *Daphnia obtusa* — quantitative genetic and
671 allozymic variation. *Genetics*, **135**(2): 367–374.
672 Sun XW, Liu DY, Zhang XF, Li WB, Liu H, Hong WG, et al. 2013. SLAF-seq: an efficient
673 method of large-scale De novo SNP discovery and genotyping using high-throughput
674 sequencing. *PloS One*, **8**(3): e58700.
675 Sundqvist L, Keenan K, Zackrisson M, Prodo¨hl P, Kleinhans D. 2016. Directional genetic
676 differentiation and relative migration. *Ecology Evolution*, **6**(11): 3461–3475.
677 Tang H, Peng J, Wang P, & Risch NJ. 2005. Estimation of individual admixture: analytical
678 and study design considerations. *Genetic Epidemiology*, **28**(4): 289–301.
679 Teng HJ, Zhang YH, Shi CM, Mao FB, Cai WS, Lu L, et al. 2017. Population genomics
680 reveals speciation and introgression between Brown norway rats and their sibling
681 species. *Molecular Biology and Evolution*, **34**(9): 2214–2228.
682 Wójcik AM, Polly PD, Sikorski MD, Wójcik JM. 2006. Selection in a cycling population:

differential response among skeletal traits. *Evolution*, **60**(9): 1925–1935.

Wulf S, Mark J, Hardiman MJ, Staff RA, Koutsodendris A, Appelt O, et al. 2018. The marine isotope stage 1–5 cryptotephra record of tenaghi philippon, greece: towards a detailed tephrostratigraphic framework for the eastern mediterranean region. *Quaternary Science Reviews*, **186**: 236–262.

Xia L, Yang QX, Ma Y, Feng ZJ, Zhou LZ. 2006. A guide to the measurement of mammal skull：Rodentia and Lagomorpha. *Chinese Journal of Zoology*, **41**(5): 668–671.

Yang QS, Xia L, Ma Y, Feng ZJ, Quan GQ. 2005. A Guide to the Measurement of mammal skull I: basic measurement. *Chinese Journal of Zoology*, **40**(3): 50–56.

Zeng T, Jin W, Sun ZY, Liu Y, Murphy RW, Fu JR, et al. 2013. Taxonomic position of *Eothenomys wardi* (Arvicolinae: Cricetidae) based on morphological and molecular analyses with a detailed description of the species. Zootaxa, **3682**(1): 85–104.

Zhang HJ, Zhang H, Qin XX, Wang ZK, Zhu WL. 2019. Geometric Morphometric analysis of skull dimensions of *Eothenomys miletus* from five areas of the Hengduan Mountains, Yunnan. *Chinese Journal of Wildlife*, **40** (01): 51–61.

Zhang LS. 2012. Palaeogeography of China: The formation of China's natural environment. Science Press, Beijing, China.

Zhang RZ. 2002. Geological events and mammalian distribution in China. *Acta Zoologica Sinica*, **48**(2): 141–153.

Zheng X, Levine D, Shen J, Gogarten SM, Laurie C, Weir BS. 2012. A high-performance computing toolset for relatedness and principal component analysis of SNP data. *Bioinformatics*, **28**(24): 3326–3328.

Zhou S, Wang X, Wang J, Xu L. 2006. A preliminary study on timing of the oldest Pleistocene glaciation in Qinghai-Tibetan plateau. *Quaternary International*, **154**(5): 44–51.

Zhou XM, Guang XM, Di S, Xu SX, Li MZ, Seim I, et al. 2018. Population genomics of finless porpoises reveal an incipient cetacean species adapted to freshwater. *Nature Communication*, **9**(1): 1276.

Zhu WL, Jia T, Lian X, Wang ZK. 2008. Evaporative water loss and energy metabolic in two small mammals, voles (*Eothenomys miletus*) and mice (*Apodemus chevrieri*) in Hengduan mountains region. *Journal of Thermal Biology*, **33**(6): 324–331.

Zhu WL, Cai JH, Lian X, Wang ZK. 2010. Adaptive character of metabolism in *Eothenomys miletus* in Hengduan mountains region during cold acclimation. *Journal of Thermal Biology*, **35**(8): 417–421.

Zhu WL, Cai JH, Xiao L, Wang ZK. 2011. Effects of photoperiod on energy intake, thermogenesis and body mass in *Eothenomys miletus* in Hengduan Mountain region. *Journal of Thermal Biology*, **36**(7): 380–385.

Zhu WL, Liu CY, Zhang CY, Wang ZK. 2013. Isolation and Polymorphic Loci of Microsatellite in *Eothenomys Miletus* (Microtinae Eothenomys). *Journal of Yunnan Normal University*, **33**(2), 63–69.

Zhu WL, Zhang H, Zhang L, Yu TT, Wang ZK. 2014. Thermogenic properties of Yunnan red-backed voles (*Eothenomys miletus*) from the Hengduan mountain region. *Animal Biology*, **64**(2): 59–73.

Zhu WL, Zhang D, Hou DM, Yang G. 2017. Roles of hypothalamic neuropeptide gene

expression in body mass regulation in *Eothenomys miletus* (Mammalia: Rodentia: Cricetidae). *The European Zoological Journal*, **84**(1), 322–333.

Table 1. The information of sample site.

Region	Sample number	Site	Altitude(m)	Annual average temperature(℃)	Precipitation(mm)	Vegetation types
DQ	29	99°03′15″E, 28°35′14″N	3459	4.7	633.7	Alpine meadow
XGLL	33	99°83′16″E, 27°90′13″N	3321	5.5	984.2	Subalpine meadow
LJ	33	100°23'30″E, 26°87'53″N	2478	12.6	975.0	Subalpine meadow and shrub
JC	33	99°75′03″E, 26°44′35″N	2219	13.9	987.3	Lobular shrub
ALS	33	100°42′49″E, 24°90′30″N	2183	19.7	597.0	Savanna Shrub and Grass

Table 2. The valve of nucleotide polymorphism ($\theta\pi$), Tajima. D, expected allele number, observed heterozygous, expected heterozygous, Nei diversity index, and polymorphysm information content (PIC), and the correlations analysis between environment factors, including altitude, annual average temperature, and latitude, with genetic diversity indexes of five *E. miletus* populations from Hengduan mountain.

Population	**DQ**	**XGLL**	**LJ**	**JC**	**ALS**	**Altitude (km)**		**Annual average temperature(°C)**		**Latitude**	
						r^2	***P* value**	r^2	***P* value**	r^2	***P* value**
Nucleotide polymorphism ($\theta\pi$)	2.75E-05	2.82E-05	2.74E-05	2.79E-05	2.94E-05	0.152	*>0.05*	0.389	*>0.05*	0.538	*>0.05*
Tajima. D	1.076	1.075	1.061	1.092	1.28	0.278	*>0.05*	0.577	*>0.05*	0.695	*>0.05*
Expected allele number	1.566	1.559	1.571	1.576	1.6	0.579	*>0.05*	0.847	*<0.05*	0.882	*<0.05*
Observed heterozygous	0.223	0.213	0.229	0.223	0.239	0.48	*>0.05*	0.708	*>0.05*	0.665	*>0.05*
Expected heterozygous	0.338	0.335	0.34	0.343	0.354	0.576	*>0.05*	0.842	*<0.05*	0.883	*<0.05*
Nei diversity index	0.345	0.341	0.347	0.349	0.36	0.566	*>0.05*	0.832	*<0.05*	0.86	*<0.05*

Polymorphysm information content (PIC)	0.273	0.271	0.274	0.276	0.284	0.533	*>0.05*	0.813	*<0.05*	0.864	*<0.05*

DQ: DeQin, XGLL: XiangGeLiLa, LJ: LiJiang, JC: JianChuan, ALS: AiLaoShan

753 Table 3. Mantel test between pairwise F_{ST} and environment distance as well as P_{ST}.

Traits	Pairwise F_{ST}		Geographic distance		Temperature distance		Altitude distance		Climate distance		Precipitation distance	
	r	***P value***	***r***	***P value***	***r***	***P value***	***r***	***P value***	***r***	***P value***	***r***	***P value***
BM	0.541	*P > 0.05*	0.546	*P > 0.05*	0.342	*P > 0.05*	0.777	*P < 0.05*	-0.014	*P > 0.05*	0.074	*P > 0.05*
BL	-0.148	*P > 0.05*	0.246	*P > 0.05*	0.102	*P > 0.05*	0.862	*P < 0.05*	0.248	*P > 0.05*	0.216	*P > 0.05*
T1L	0.243	*P > 0.05*	0.287	*P > 0.05*	0.219	*P > 0.05*	0.812	*P < 0.05*	0.171	*P > 0.05*	0.248	*P > 0.05*
T2L	0.455	*P > 0.05*	0.170	*P > 0.05*	0.475	*P > 0.05*	0.133	*P > 0.05*	0.274	*P > 0.05*	0.430	*P > 0.05*
CW	0.354	*P > 0.05*	0.613	*P > 0.05*	0.372	*P > 0.05*	0.929	*P < 0.05*	0.079	*P > 0.05*	0.151	*P > 0.05*
CD	-0.211	*P > 0.05*	0.444	*P > 0.05*	0.433	*P > 0.05*	0.305	*P > 0.05*	0.506	*P > 0.05*	0.405	*P > 0.05*
EL	0.742	*P > 0.05*	0.477	*P > 0.05*	0.654	*P < 0.05*	0.248	*P > 0.05*	-0.098	*P > 0.05*	0.060	*P > 0.05*
EW	-0.025	*P > 0.05*	0.390	*P > 0.05*	0.473	*P > 0.05*	-0.034	*P > 0.05*	0.370	*P > 0.05*	0.290	*P > 0.05*
FLL	-0.125	*P > 0.05*	0.321	*P > 0.05*	-0.030	*P > 0.05*	0.810	*P < 0.05*	0.382	*P > 0.05*	0.406	*P > 0.05*
HLL	0.168	*P > 0.05*	-0.108	*P > 0.05*	-0.118	*P > 0.05*	-0.086	*P > 0.05*	-0.643	*P < 0.05*	-0.737	*P < 0.05*

CL	0.886	*P < 0.01*	0.687	*P < 0.05*	0.588	*P > 0.05*	0.296	*P > 0.05*	-0.754	*P < 0.05*	-0.704	*P < 0.05*
CBL	0.797	*P > 0.05*	0.524	*P > 0.05*	0.443	*P > 0.05*	0.493	*P > 0.05*	-0.254	*P > 0.05*	-0.108	*P > 0.05*
CH	0.209	*P > 0.05*	0.010	*P > 0.05*	-0.012	*P > 0.05*	0.447	*P > 0.05*	-0.028	*P > 0.05*	0.011	*P > 0.05*
PNL	0.362	*P > 0.05*	-0.034	*P > 0.05*	0.042	*P > 0.05*	0.214	*P > 0.05*	-0.040	*P > 0.05*	-0.008	*P > 0.05*
ZB	-0.171	*P > 0.05*	-0.459	*P > 0.05*	-0.665	*P > 0.05*	-0.055	*P > 0.05*	-0.055	*P > 0.05*	0.004	*P > 0.05*
NW	-0.015	*P > 0.05*	-0.162	*P > 0.05*	0.130	*P > 0.05*	-0.441	*P > 0.05*	-0.514	*P > 0.05*	-0.550	*P > 0.05*
CCL	0.412	*P > 0.05*	0.317	*P > 0.05*	0.265	*P > 0.05*	0.297	*P > 0.05*	-0.612	*P > 0.05*	-0.679	*P > 0.05*
IB	-0.29	*P > 0.05*	0.179	*P > 0.05*	0.025	*P > 0.05*	0.861	*P < 0.05*	0.348	*P > 0.05*	0.285	*P > 0.05*
ESL	-0.462	*P > 0.05*	-0.270	*P > 0.05*	-0.405	*P > 0.05*	-0.147	*P > 0.05*	0.475	*P > 0.05*	0.395	*P > 0.05*
AVL	0.715	*P > 0.05*	0.472	*P > 0.05*	0.778	*P < 0.05*	-0.147	*P > 0.05*	-0.468	*P > 0.05*	-0.449	*P > 0.05*
UTRL	0.414	*P > 0.05*	0.253	*P > 0.05*	0.130	*P > 0.05*	0.715	*P < 0.05*	0.063	*P > 0.05*	0.182	*P > 0.05*
LTRL	0.147	*P > 0.05*	0.011	*P > 0.05*	-0.025	*P > 0.05*	-0.202	*P > 0.05*	0.142	*P > 0.05*	0.186	*P > 0.05*

754 BM: Body mass, BL: body length, T_1L: tail length, T_2L: torso length, CW: chest width, CD: chest depth, EL: ear length, EW: ear width, FLL:

755 fore limb length, HLL: hind limb length, CL: cranial length, CBL: cranial basal length, CH: cranial height, PNL: pillow nose length, ZB:
756 zygomatic breadth, NW: neurocranium width, CCL: covering cap length, IB: interorbital breadth, ESL: eye socket length, AVL: auditory vesicle
757 length, UTRL: upper tooth row length and LTRL: lower tooth row length. Data were analyzed by Mantel test.
758
759
760
761
762
763
764

765 **Figure Legends**

766 **Figure 1** Population structure. (A) Sampling information of *E. miletus* used in this
767 study. (B) Genetic structure of the 161 individuals from five populations. Groupings
768 of samples from 1–10 ancestral clusters are shown. Groupings of samples from one to
769 ten ancestral clusters are shown. (C) Scatter plot of principal components 1 versus 2
770 (PC1 versus PC2 showed in left) and principal components 1 versus 3 (PC1 versus
771 PC3 showed in right) for the five populations. (D) Neighboring-joining phylogenetic
772 tree of five populations. DQ: DeQin, XGLL: XiangGeLiLa, LJ: LiJiang, JC:
773 JianChuan, ALS: AiLaoShan.

774 **Figure 2** Demographic history and gene flow of *E. miletus*. (A) Diagram of relative
775 magnitude and direction of gene flow. Arrowheads show the estimated direction of
776 gene flow. (B) Demographic history inferred by PSMC. The major stage, the
777 Quaternary glaciation (3000~10 Ka BP), includes twice increase (2000Kya and 90kya)
778 and twice decrease (Marine Isotope Stage 12 (500Ka ± 5Ka BP) and Marine Isotope
779 Stage 3 (60Ka-25Ka BP)). DQ: DeQin, XGLL: XiangGeLiLa, LJ: LiJiang, JC:
780 JianChuan, ALS: AiLaoShan.

781 **Figure 3** Genetic differentiation and linear regression lines showing the correlations
782 among genetic, geographic, and environmental distances. (A) The heat map of
783 pairwise F_{ST} between *E. miletus* populations, Groups: DQ: DeQin population, XGLL:
784 XiangGeLiLa population, LJ: LiJiang population, JC: JianChuan population, ALS:
785 AiLaoShan population. Mantel test between pairwise F_{ST} and $F_{ST}/(1-F_{ST})$ as well as
786 geographic distance (IBD: B, C), temperature distance (IBT: D, E), altitude distance

787 (IBA: F, G), climate distance (IBC: H, I), and precipitation distance (IBP: G, K). Data
788 were analyzed by Mantel test. $P < 0.05$. (L) RDA ordination ts of genetic diversity in
789 *E. miletus*.

790 **Figure 4** Group differences in body mass (A) and twenty-one phenotypic traits (B) of
791 five *E. miletus* populations from HM region. Data were analyzed by one-way ANOVA
792 followed by the LSD post-hoc test. Significant differences were indicated by different
793 alphabetic letters. One-way clustering heat map based on the body and skull traits in *E.*
794 *miletus* (C). The correlation matrix between altitude, annual average temperature and
795 latitude with twenty-two phenotypic traits (D). DQ: DeQin, XGLL: XiangGeLiLa, LJ:
796 LiJing, JC: JianChuan, ALS: AiLaoShan; BM: Body mass, BL: body length, T_1L: tail
797 length, T_2L: torso length, CW: chest width, CD: chest depth, EL: ear length, EW: ear
798 width, FLL: fore limb length, HLL: hind limb length, CL: cranial length, CBL: cranial
799 basal length, CH: cranial height, PNL: pillow nose length, ZB: zygomatic breadth,
800 NW: neurocranium width, CCL: covering cap length, IB: interorbital breadth, ESL:
801 eye socket length, AVL: auditory vesicle length, UTRL: upper tooth row length and
802 LTRL: lower tooth row length.

803 **Figure 5** Two-way clustering heat map of the value of pairwise P_{ST} vs F_{ST} value
804 between five *E. miletus* populations from Hengduan mountain regions. DQ: DeQin,
805 XGLL: XiangGeLiLa, LJ: LiJiang, JC: JianChuan, ALS: AiLaoShan; BM: Body mass,
806 BL: body length, T_1L: tail length, T_2L: torso length, CW: chest width, CD: chest depth,
807 EL: ear length, EW: ear width, FLL: fore limb length, HLL: hind limb length, CL:
808 cranial length, CBL: cranial basal length, CH: cranial height, PNL: pillow nose length,

809 ZB: zygomatic breadth, NW: neurocranium width, CCL: covering cap length, IB:
810 interorbital breadth, ESL: eye socket length, AVL: auditory vesicle length, UTRL:
811 upper tooth row length and LTRL: lower tooth row length.

812 **Figure 6** The heat map of comparison value between P_{ST} estimated by phenotypic
813 measures using four different heritability estimates (0.25 (A), 0.5 (B), 0.75 (C) and 1
814 (D)), based on the assumptions that there is no environmental variance, and pairwise
815 F_{ST} calculated using differentiation at neutral molecular markers. DQ: DeQin, XGLL:
816 XiangGeLiLa, LJ: LiJiang, JC: JianChuan, ALS: AiLaoShan; BM: Body mass, BL:
817 body length, T_1L: tail length, T_2L: torso length, CW: chest width, CD: chest depth, EL:
818 ear length, EW: ear width, FLL: fore limb length, HLL: hind limb length, CL: cranial
819 length, CBL: cranial basal length, CH: cranial height, PNL: pillow nose length, ZB:
820 zygomatic breadth, NW: neurocranium width, CCL: covering cap length, IB:
821 interorbital breadth, ESL: eye socket length, AVL: auditory vesicle length, UTRL:
822 upper tooth row length and LTRL: lower tooth row length.

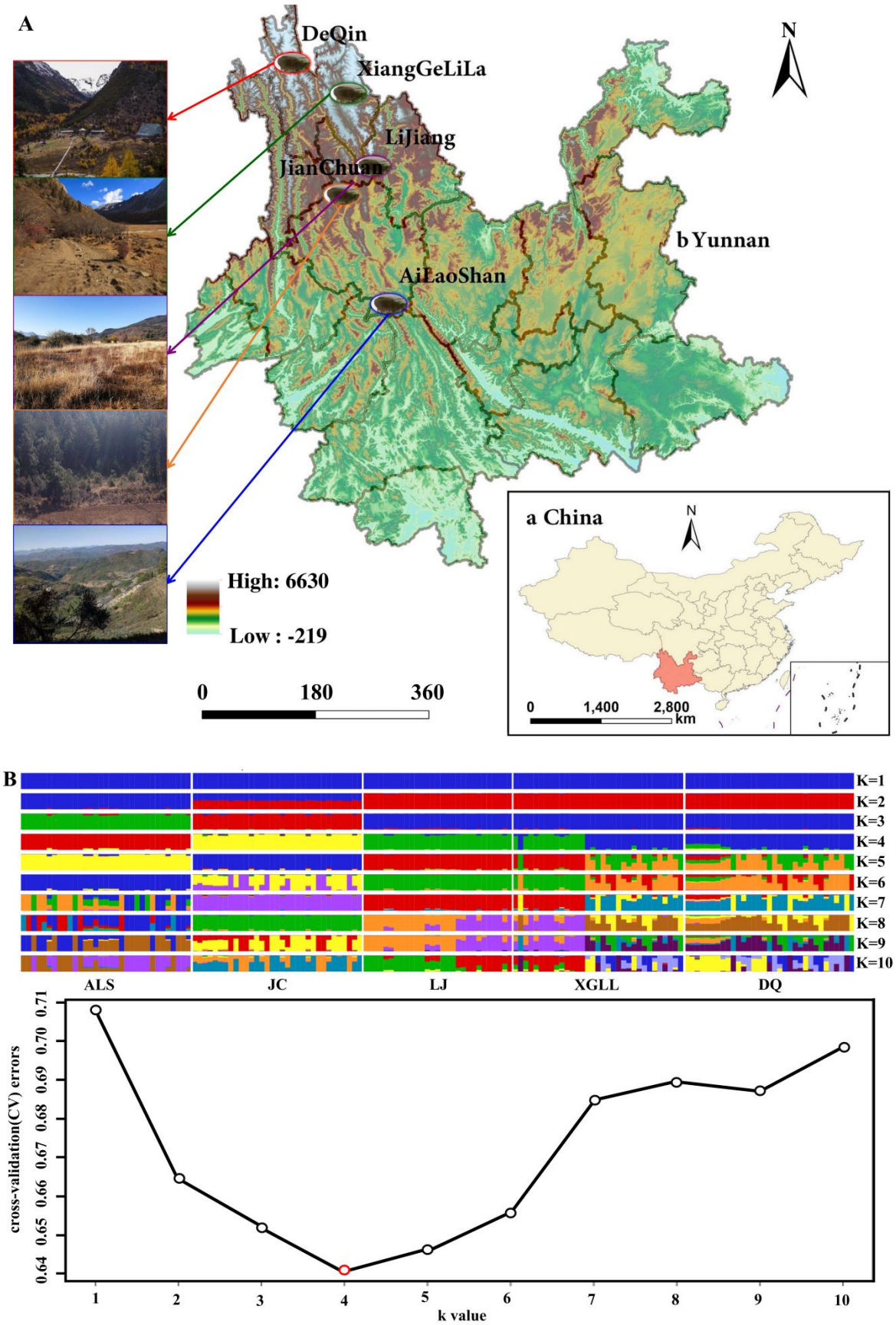
A
DeQin
XiangGeLiLa
LiJiang
JianChuan
AiLaoShan
b Yunnan
N
High: 6630
Low : -219
0
180
360
a China
N
0
1,400
2,800
km
B
K=1
K=2
K=3
K=4
K=5
K=6
K=7
K=8
K=9
K=10
ALS
JC
LJ
XGLL
DQ
cross-validation(CV) errors
0.64
0.65
0.66
0.67
0.68
0.69
0.70
0.71
1
2
3
4
5
6
7
8
9
10
k value

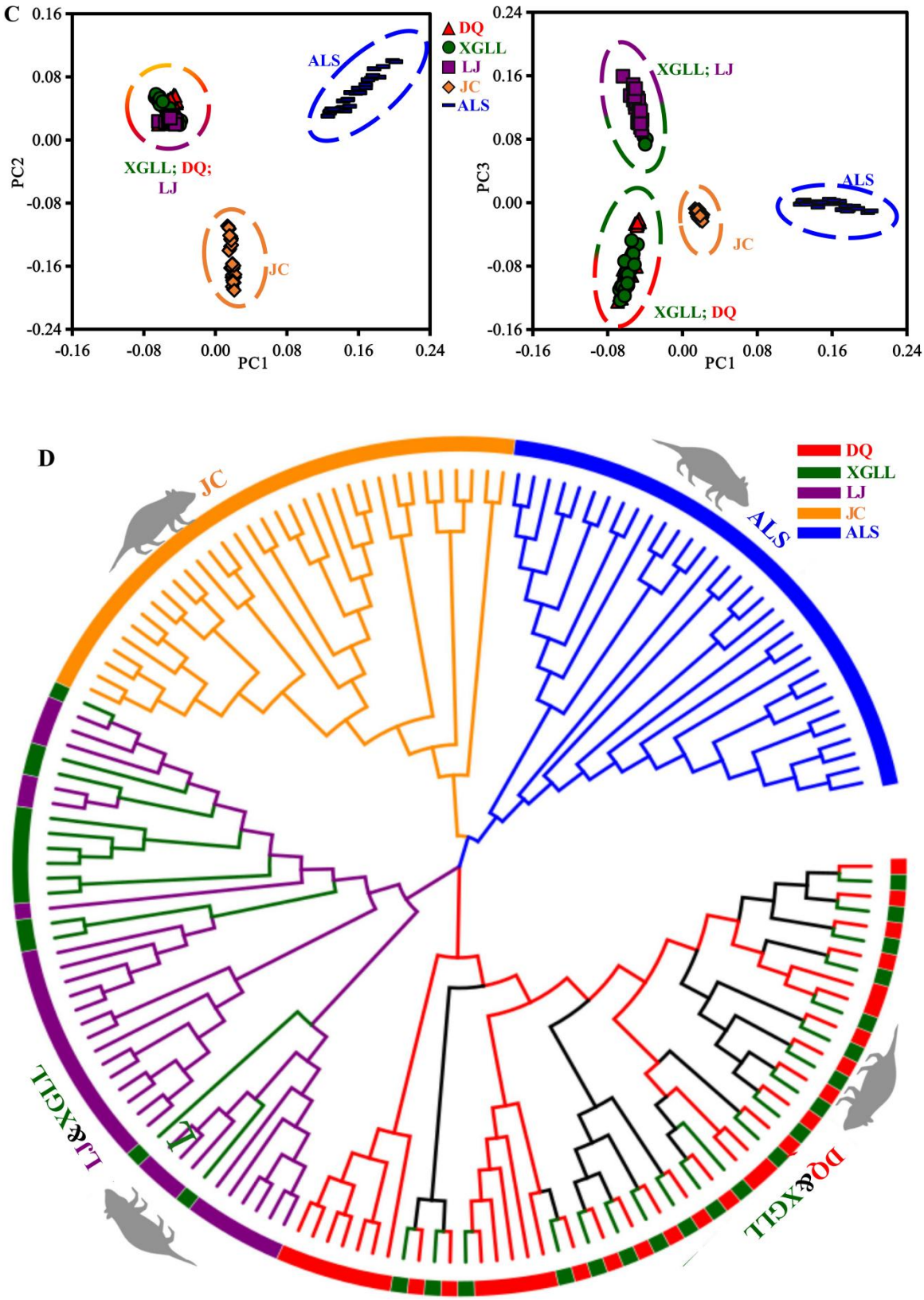
C
PC2
PC1
PC3
DQ
XGLL
LJ
JC
ALS
XGLL; DQ; LJ
XGLL; LJ
XGLL; DQ
D
JC
ALS
LJ&XGLL
DQ&XGLL
LJ

Figure 1

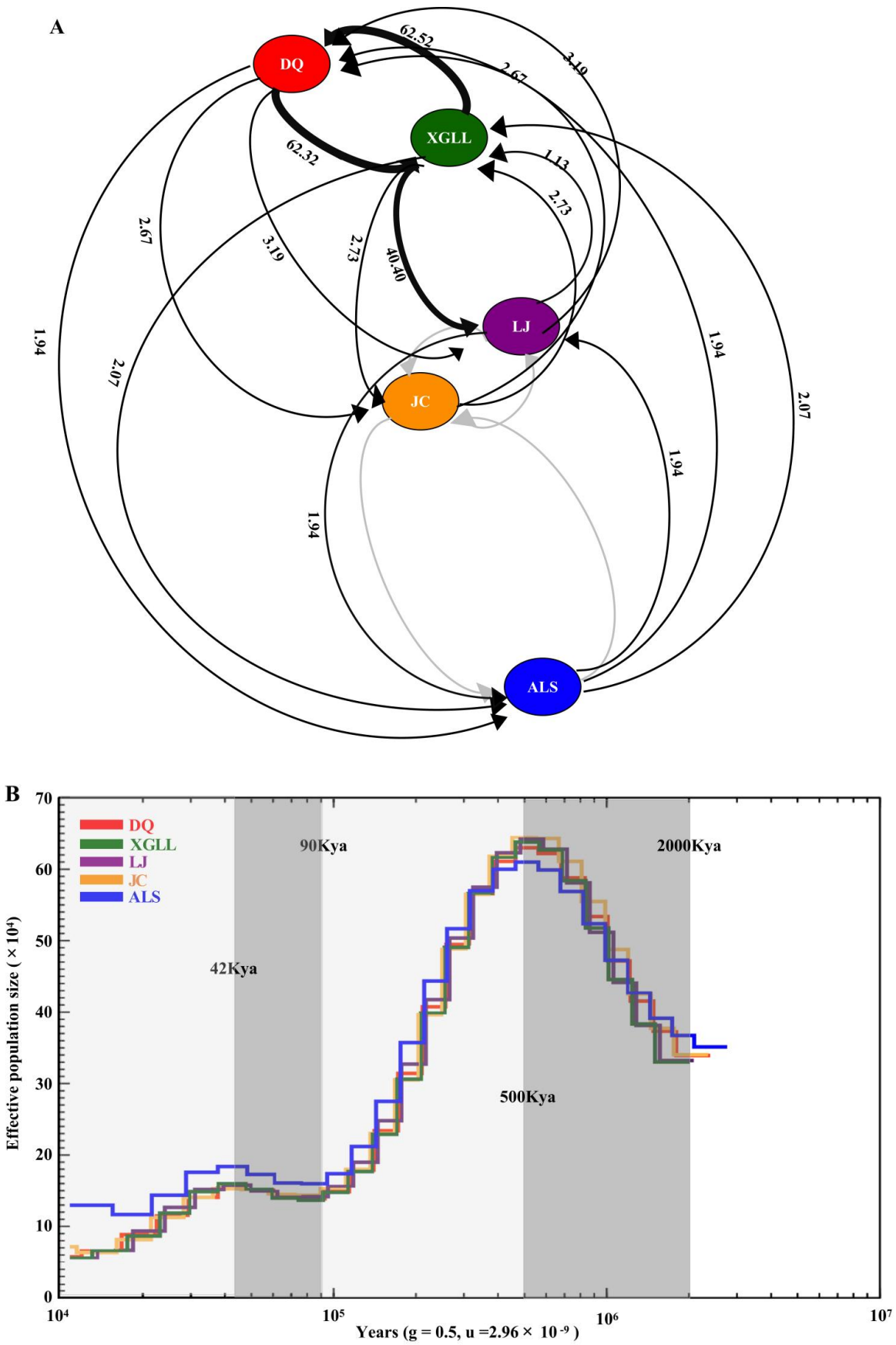
A
DQ
XGLL
LJ
JC
ALS
62.52
62.32
40.40
3.19
2.67
2.73
1.13
1.94
2.07
B
DQ
XGLL
LJ
JC
ALS
90Kya
2000Kya
42Kya
500Kya
Effective population size (× 10⁴)
Years (g = 0.5, u =2.96 × 10 -9)

Figure 2

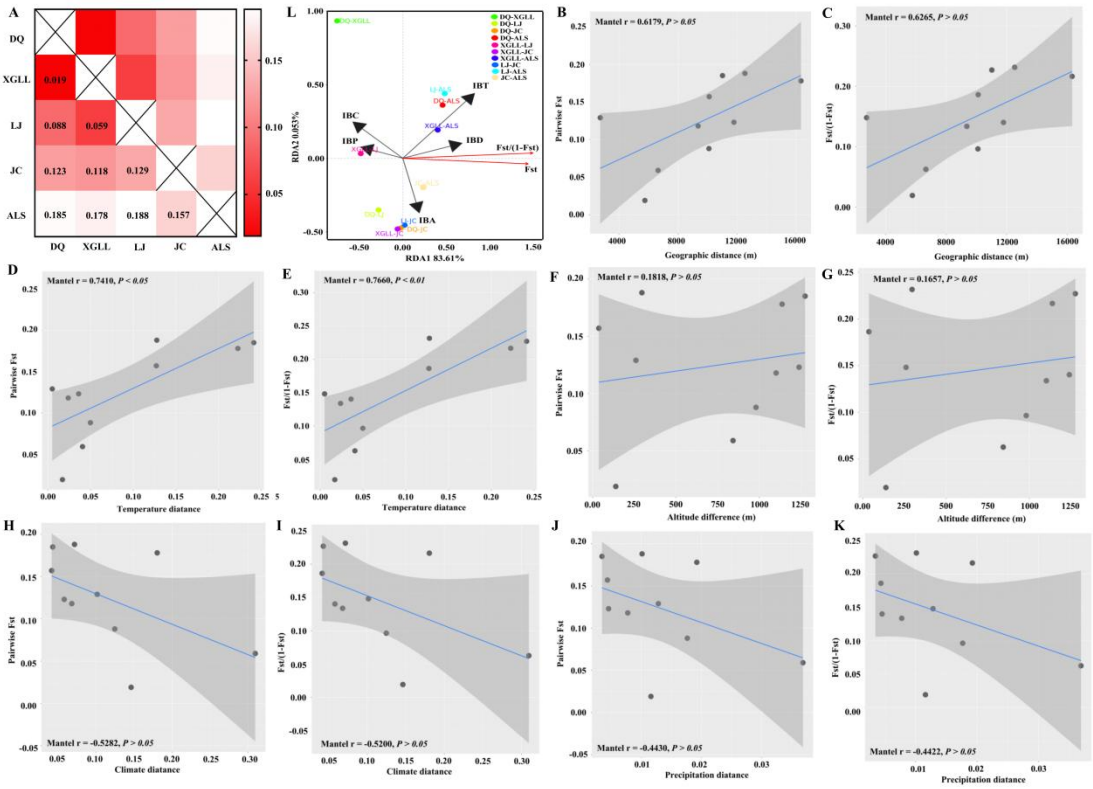
A
DQ
XGLL
LJ
JC
ALS
0.019
0.088
0.059
0.123
0.118
0.129
0.185
0.178
0.188
0.157
L
DQ-XGLL
DQ-LJ
DQ-JC
DQ-ALS
XGLL-LJ
XGLL-JC
XGLL-ALS
LJ-JC
LJ-ALS
JC-ALS
IBT
IBC
IBP
IBD
IBA
Fst/(1-Fst)
Fst
RDA1 83.61%
RDA2 0.053%
B
Mantel r = 0.6179, P > 0.05
Pairwise Fst
Geographic distance (m)
C
Mantel r = 0.6265, P > 0.05
Fst/(1-Fst)
Geographic distance (m)
D
Mantel r = 0.7410, P < 0.05
Pairwise Fst
Temperature diatance
E
Mantel r = 0.7660, P < 0.01
Fst/(1-Fst)
Temperature diatance
F
Mantel r = 0.1818, P > 0.05
Pairwise Fst
Altitude difference (m)
G
Mantel r = 0.1657, P > 0.05
Fst/(1-Fst)
Altitude difference (m)
H
Mantel r = -0.5282, P > 0.05
Pairwise Fst
Climate diatance
I
Mantel r = -0.5200, P > 0.05
Fst/(1-Fst)
Climate diatance
J
Mantel r = -0.4430, P > 0.05
Pairwise Fst
Precipitation diatance
K
Mantel r = -0.4422, P > 0.05
Fst/(1-Fst)
Precipitation diatance

Figure 3

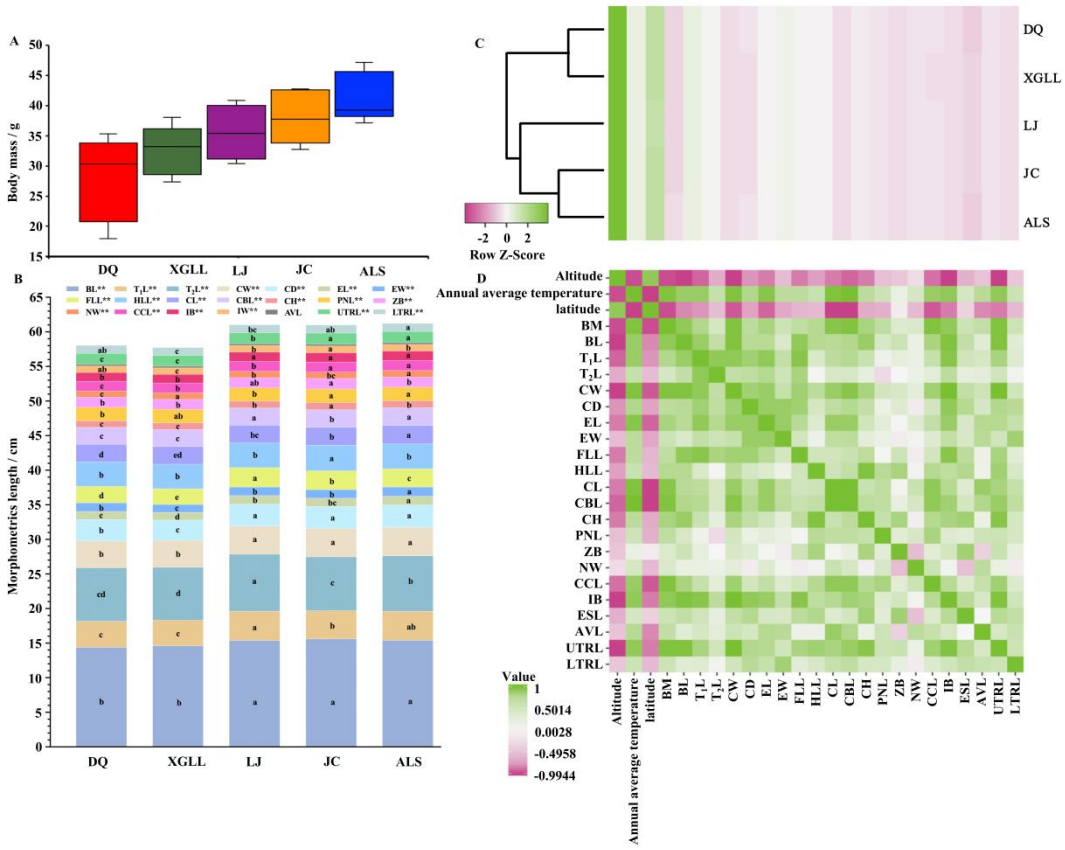
A
Body mass / g
DQ
XGLL
LJ
JC
ALS
B
Morphometrics length / cm
C
Row Z-Score
D
Value
1
0.5014
0.0028
-0.4958
-0.9944
Altitude
Annual average temperature
latitude
BM
BL
CW
CD
EL
EW
FLL
HLL
CL
CBL
CH
PNL
ZB
NW
CCL
IB
ESL
AVL
UTRL
LTRL

Figure 4

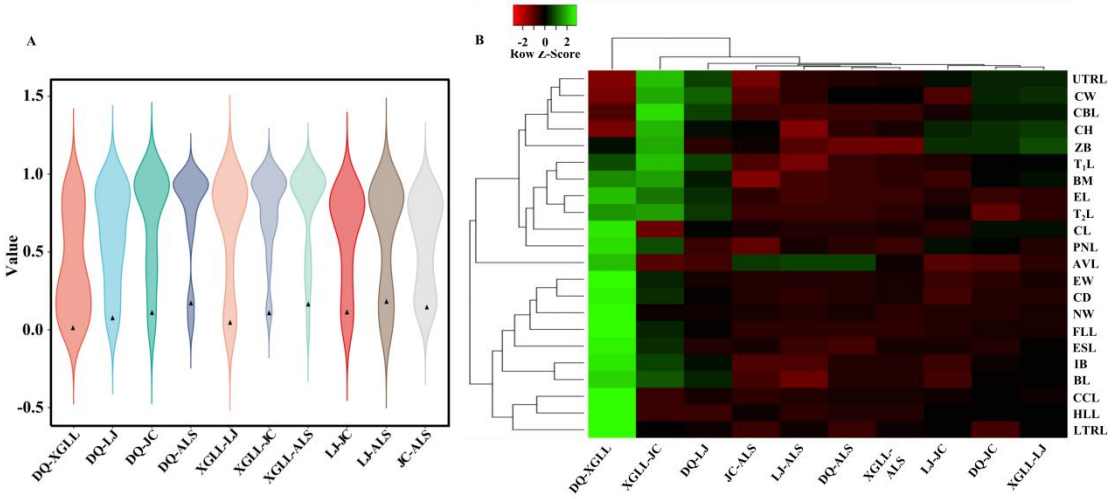
A
B
Value
1.5
1.0
0.5
0.0
-0.5
DQ-XGLL
DQ-LJ
DQ-JC
DQ-ALS
XGLL-LJ
XGLL-JC
XGLL-ALS
LJ-JC
LJ-ALS
JC-ALS
-2 0 2
Row Z-Score
UTRL
CW
CBL
CH
ZB
T1L
BM
EL
T2L
CL
PNL
AVL
EW
CD
NW
FLL
ESL
IB
BL
CCL
HLL
LTRL
DQ-XGLL
XGLL-JC
DQ-LJ
JC-ALS
LJ-ALS
DQ-ALS
XGLL-ALS
LJ-JC
DQ-JC
XGLL-LJ

Figure 5

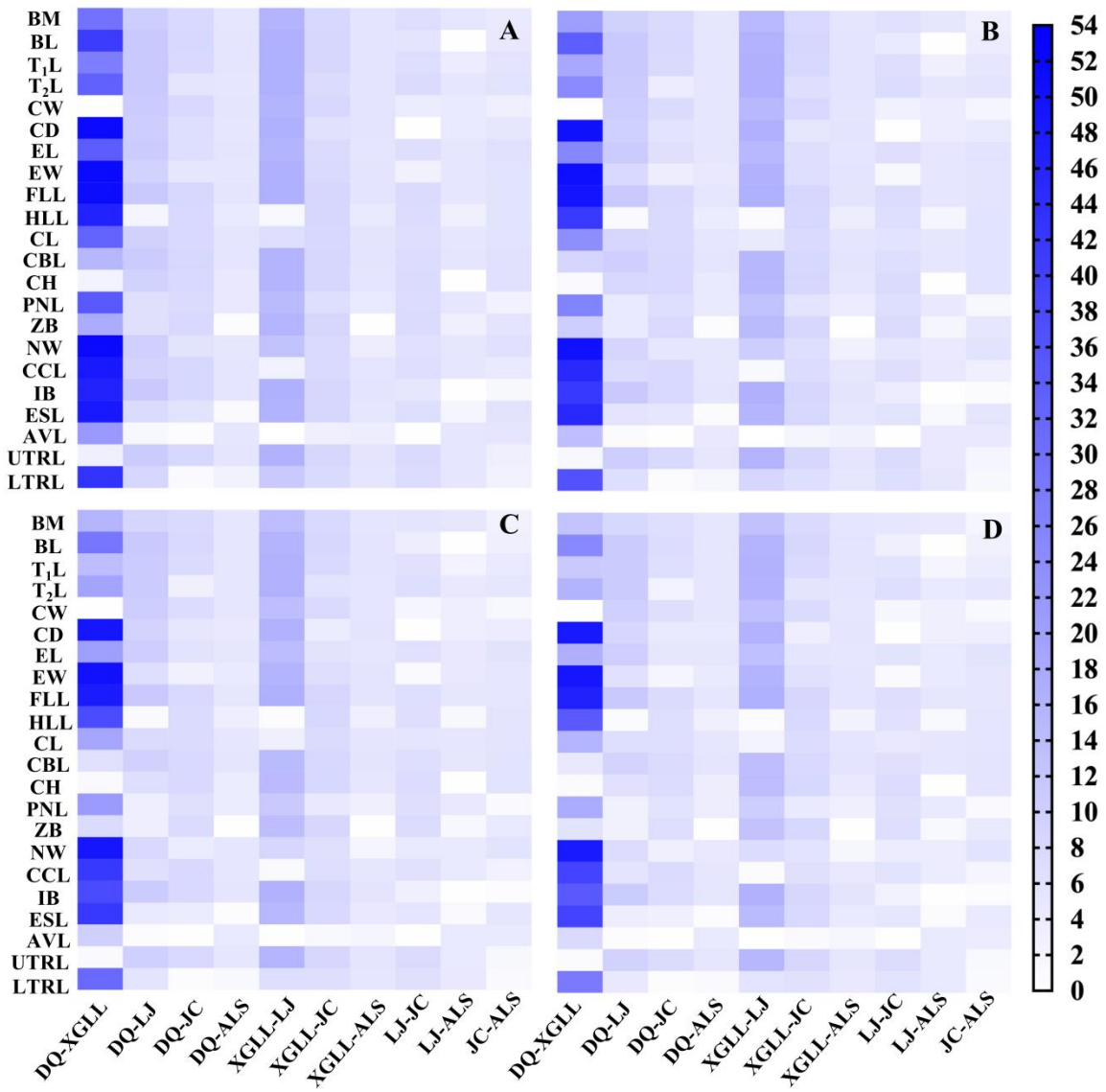
A
B
C
D
BM
BL
T1L
T2L
CW
CD
EL
EW
FLL
HLL
CL
CBL
CH
PNL
ZB
NW
CCL
IB
ESL
AVL
UTRL
LTRL
DQ-XGLL
DQ-LJ
DQ-JC
DQ-ALS
XGLL-LJ
XGLL-JC
XGLL-ALS
LJ-JC
LJ-ALS
JC-ALS
54
52
50
48
46
44
42
40
38
36
34
32
30
28
26
24
22
20
18
16
14
12
10
8
6
4
2
0

Figure 6